IEEE Access
Multidisciplinary | Rapid Review | Open Access Journal

Received December 19, 2018, accepted December 28, 2018, date of publication January 11, 2019, date of current version February 8, 2019.

Digital Object Identifier 10.1109/ACCESS.2019.2892414

Proportional Retarded Control of Robot Manipulators

MARIO RAMÍREZ-NERIA[1], GILBERTO OCHOA-ORTEGA[2], ALBERTO LUVIANO-JUÁREZ[3], NORMA LOZADA-CASTILLO[3], MIGUEL ANGEL TRUJANO-CABRERA[2], AND JUAN PABLO CAMPOS-LÓPEZ[2]

[1]Departamento de Mecatrónica, Universidad Tecnológica de México, UNITEC Campus Atizapán, Atizapán de Zaragoza 52999, Mexico
[2]Departamento de Mecatrónica, Universidad Politécnica del Valle de México, Tultitlán de Mariano Escobedo 54910, Mexico
[3]Instituto Politécnico Nacional-UPIITA, Mexico City 07340, Mexico

Corresponding author: Gilberto Ochoa-Ortega (gochoa79@gmail.com)

The work of A. Luviano-JuÁrez and N. Lozada-Castillo was supported in part by SIP-IPN under Grant SIP20181665 and Grant SIP20181146.

ABSTRACT In the present contribution, a methodology to solve the tracking control problem of robot manipulators through the use of a Proportional Retarded plus Gravity (PR+G) compensation scheme is presented. The main advantage of the proposal is to avoid the necessity of velocity measurements or their estimation, which is commonly used in most control schemes, such as the proportional derivative-type controllers or the computed torque control. The design of the PR+G controller is addressed via σ-stability analysis and its performance is tested in an experimental platform that consists of 2 degrees of the freedom robot manipulator. The proposed controller is compared with a classic proportional derivative plus gravity compensation scheme. The results are analyzed from a frequency perspective and measured by a quadratic error index.

INDEX TERMS Manipulator robot, time-delay controller, trajectory tracking.

I. INTRODUCTION

Regulation and tracking control problems of flexible and rigid robot manipulators have been presented in literature, where the majority of those proposals used the proportional-derivative feedback or the computed torque algorithm as controllers, which are based on the assumption that the information of the complete state is available, see [1]–[9], and references therein. However, this assumption in practice is partially fulfilled, mainly because the signal may not be available for measurement and therefore it should be determined by a first-order numerical differentiation or some other approach. Due to the interest of avoiding the use of velocity measurements, different methods have been developed [10]–[15] that, in general, follow a two-step design procedure:

a) Construct an observer for the velocity signal employing the available inputs and outputs,
b) Design a state feedback controller where the velocity is replaced by the one reconstructed from the observer.

However, these solutions only rely on local stability and measurement noises can reduce the quality of the velocity estimation, among other arising problems.

Time delay may appear inherently present in a wide class of systems. The effects of time delay have been an active area of a scientific research in a wide rank of sciences for example biological, ecological, engineering systems, etc [16]–[20]. The analysis of this class of systems has come up with an important amount of theoretical contributions in the area of stability analysis.

In controlled dynamic systems, time delays can arise due to communication effects, or natural phenomena, [21]–[23], whose dynamic effects cannot be neglected. In one hand, the presence of time delays may lead to poor performance or in some cases instability. On the other hand, the introduction of time delays for control proposes can improve the system performance or even stabilize it [24]. This approach has been used successfully solving the problem of stabilizing chaotic and oscillatory second order systems [25]. The stabilizing effect of delays in feedback has been studied in depth using the σ-stability [26] for Linear Matrix Inequalities (LMI) [27].

The Proportional Retarded (PR) controller is a recently introduced approach [28] that can be an alternative of classic Proportional Derivative control laws. This scheme avoids the use of state observers or numerical differentiation, which also enhances the system response against noisy measurements. However, the main disadvantage of this scheme is the fact that it implies a careful stability analysis to compensate the

introduction of the resulting infinite dimensional closed loop system. To overcome this fact, it has been studied detailed in frequency domain analysis of the σ-stability for a second order linear system [29], [30]. As main result of this study, a tuning methodology of PR controllers was developed, also experimental results were achieved using a PR control law solving the problem of trajectory tracking position of a second order linear system, PR controller performance has showed advantages respect a Proportional Derivative (PD) controller, for example: easy implementation in a real-time process, and reduction of noise of control signal.

Some applications of the PR control deal with linear or approximately linearized systems which work mainly on an equilibrium zone [31]. In other applications like robot control in trajectory tracking tasks, the operation conditions demand a larger operation zone of the controllers, and it has been shown that PD controllers can stabilize robotic systems of open kinematic chain structure [2]. For this instance, it is motivating the use of PR controllers as a practical alternative of robotic control designs.

In the present manuscript, a proportional retarded controller is proposed to perform trajectory tracking tasks of robotic systems of nonlinear nature. Furthermore, to deal with the larger operation zone demanded by the control of robotic manipulators a gravity compensation scheme is included in the proportional retarded controller. Even when the main proposal deals with general systems, for implementation purposes, a two degrees of freedom robotic manipulator is considered. To the best of the authors' knowledge, this is the first instance this scheme has been applied to a nonlinear system without explicitly linearizing it. The natural properties of this class of systems allow to establish operation bounds, leading to a linear dominant dynamics affected by a set of bounded lumped disturbances. Thus, an ultimate bound tracking can be shown by means of the dominant roots of the linear dominant delayed dynamics. For comparison purposes, a PD plus gravity compensator controller is also considered. The rest of the article is organized as follows: Section II presents the mathematical model of the robotic system, the problem formulation and the hypotheses for the control design. Section III describes the PR control design and establishes the error dynamics stability in terms of a disturbed delayed linear dominant dynamics. Section IV-A describe the dynamic models of the 2-DOF robot manipulator. Section IV-C is devoted to the design of the proposed controls schemes (PR+G and PD+G), while the details of the laboratory prototype, as well as the corresponding experimental results are given in Section V. Finally, a brief analysis of the results and the conclusions are given in Section VI.

Notation: Given a vector $\mathbf{x} \in \mathbb{R}^n$, $\mathbf{x}^\intercal$ denotes its transpose and the euclidean norm of vector $\mathbf{x}$ is defined as $\|\mathbf{x}\| = \sqrt{\mathbf{x}^T\mathbf{x}}$. Let $\mathbf{A} \in^{n\times n}$, then the induced matrix norm is given by $\|\mathbf{A}\| = \sqrt{\lambda_M\left\{\mathbf{A}^T\mathbf{A}\right\}}$ where $\lambda_M\{\cdot\}$ represents the maximum eigenvalue of the matrix.

II. PRELIMINARIES AND PROBLEM FORMULATION

A. PRELIMINARIES

The general dynamic model of a fully actuated manipulator robot can be obtained by using either, the Euler-Lagrange or Newton-Euler formalism [2]. This class of systems is commonly expressed as follows:

$$\mathbf{M}(\mathbf{q})\ddot{\mathbf{q}} + \mathbf{C}(\mathbf{q},\dot{\mathbf{q}})\dot{\mathbf{q}} + \mathbf{G}(\mathbf{q}) = \tau - \tau_{\mathbf{d}} - \mathbf{D}\dot{\mathbf{q}}, \tag{1}$$

where $\mathbf{q} \in \mathbb{R}^n$ is the joint variable vector, $\tau \in \mathbb{R}^n$ is the control torque vector and $\tau_{\mathbf{d}} \in \mathbb{R}^n$ is the disturbance vector that contains the unmodeled dynamics and external disturbance inputs. $\mathbf{M}(\mathbf{q}) \in \mathbb{R}^{n\times n}$ represents the manipulator inertia matrix, $\mathbf{C}(\mathbf{q},\dot{\mathbf{q}}) \in \mathbb{R}^{n\times n}$ corresponds to the Coriolis and centripetal forces matrix and $\mathbf{G}(\mathbf{q}) \in \mathbb{R}^n$ is the gravitational forces vector. The viscous friction is denoted by a diagonal matrix $\mathbf{D} \in \mathbb{R}^{n\times n}$.

Under the assumption that matrices $\mathbf{M}(\mathbf{q})$, $\mathbf{C}(\mathbf{q},\dot{\mathbf{q}})$ and $\mathbf{G}(\mathbf{q})$ are perfectly known, then, there exist positive constants $\kappa_m, \kappa_M, \kappa_C, \kappa_G, \gamma, d \in \mathbb{R}^+$ that satisfy the following relations [2], [32]–[34]:

$$\kappa_m \leq \|\mathbf{M}(\mathbf{q})\| \leq \kappa_M, \tag{2}$$

$$\|\mathbf{C}(\mathbf{q},\dot{\mathbf{q}})\dot{\mathbf{q}}\| \leq \kappa_C \|\dot{\mathbf{q}}\|^2, \tag{3}$$

$$\|\mathbf{G}(\mathbf{q})\| \leq \kappa_G, \tag{4}$$

$$\|\tau_{\mathbf{d}}\| \leq \gamma, \tag{5}$$

$$\|D\| \leq d. \tag{6}$$

By defining the reference trajectory as $\mathbf{q}^*$, then the tracking error is defined as:

$$\mathbf{e}_{\mathbf{q}} = \mathbf{q}^* - \mathbf{q}. \tag{7}$$

Since the inertia matrix is invertible, the open loop tracking error dynamics due to the robot dynamics can be expressed as:

$$\ddot{\mathbf{e}}_{\mathbf{q}} = \ddot{\mathbf{q}}^* + \mathbf{M}(\mathbf{q})^{-1}\left[\mathbf{C}(\mathbf{q},\dot{\mathbf{q}})\dot{\mathbf{q}} + \mathbf{G}(\mathbf{q}) + \mathbf{D}\dot{\mathbf{q}} + \tau_{\mathbf{d}} - \tau\right]. \tag{8}$$

Now, if we assume that all states can be measured, the following control (computed torque τ_{CT}), can be proposed:

$$\tau_{CT} = \mathbf{M}(\mathbf{q})(\ddot{\mathbf{q}}^* - \mathbf{u}_{CT}) + [\mathbf{C}(\mathbf{q},\dot{\mathbf{q}}) + \mathbf{D}]\dot{\mathbf{q}} + \mathbf{G}(\mathbf{q}). \tag{9}$$

Here $\mathbf{u}_{CT} \in \mathbb{R}^n$ is a control input for the closed loop system. Thus, substituting (9) into (8), the error dynamics, are reduced to:

$$\ddot{\mathbf{e}}_{\mathbf{q}} = \mathbf{u}_{CT} + \mathbf{W}_{\mathbf{p}}, \tag{10}$$

where the term $\mathbf{W}_{\mathbf{p}} \in \mathbb{R}^n$, defined as $\mathbf{W}_{\mathbf{p}} = \mathbf{M}(\mathbf{q})^{-1}\tau_{\mathbf{d}}$ represents the unmodeled dynamics.

B. CONTROL PROBLEM FORMULATION

Given the dynamics (1), it is desired to track the reference trajectory $\mathbf{q}^*$. To solve this problem using the control law (9), both the joint variable vector $\mathbf{q}$ and its time-derivative $\dot{\mathbf{q}}$ must be available for measurement. The problem is that, in many practical implementations, the velocity vector $\dot{\mathbf{q}}$ cannot be

measured directly. Some common strategies for the estimation of the derivative of vector $\mathbf{q}$ are the use of state observers, numerical approximations, filter processing, implementation of analog tachometer sensors, among others (see, [10], [11], [15], [35]–[37]). The disadvantage of using those techniques is the addition of noise to the computed torque control law (see, [38]–[41]) and, as a consequence, the proposed control law (9) is not recommended in real-time applications. Hence, under these considerations the control problem formulation, relies on the design of an output-feedback control law, that minimizes or even avoids, the use of the time derivative $\dot{\mathbf{q}}$.

In the present proposal, avoiding the use of velocity measurements, it is desired to cancel out the gravity vector $\mathbf{G}(\mathbf{q})$, thus, the computed torque control in (9) becomes in the form:

$$\tau = \mathbf{M}(\mathbf{q})\left(\ddot{\mathbf{q}}^* - \mathbf{u}\right) + \mathbf{G}(\mathbf{q}), \tag{11}$$

then, substituting (11) into (8) yields the new closed loop error dynamics as:

$$\ddot{\mathbf{e}}_\mathbf{q} = \mathbf{u} + \mathbf{W_{cd}}, \tag{12}$$

where:

$$\mathbf{W_{cd}} = \mathbf{M}(\mathbf{q})^{-1}\left[(\mathbf{C}(\mathbf{q},\dot{\mathbf{q}}) + \mathbf{D})\dot{\mathbf{q}} + \tau_\mathbf{d}\right], \tag{13}$$

includes the viscous friction forces and the Coriolis and centripetal terms. Here, the following assumption is considered [42], [43]:

Assumption 1: The term $\mathbf{W_{cd}}$ can be approximated by a time-dependent Taylor polynomial of the form:

$$\mathbf{W_{cd}} = \begin{bmatrix} \alpha_{10} + \alpha_{11}t + \cdots + \alpha_{1m}t^m + H.O.T. \\ \alpha_{20} + \alpha_{21}t + \cdots + \alpha_{2m}t^m + H.O.T. \\ \vdots \\ \alpha_{n0} + \alpha_{n1}t + \cdots + \alpha_{nm}t^m + H.O.T. \end{bmatrix}. \tag{14}$$

III. PROPORTIONAL RETARDED PLUS GRAVITY COMPENSATOR CONTROLLER

In the present section, in order to avoid using the velocity joint vector $\dot{\mathbf{q}}$, a Proportional Retarded control scheme (see, [29], [30]) and is denoted by:

$$\mathbf{u} = \mathbf{u_{PR}} = -\mathbf{K_P}\mathbf{e_q} + \mathbf{K_R}\mathbf{e_q}(t - T_i). \tag{15}$$

Here

$$\mathbf{e_q}(t - T_i) = \begin{bmatrix} e_{q1}(t - T_1) \\ e_{q2}(t - T_2) \\ \vdots \\ e_{qn}(t - T_n) \end{bmatrix} = \begin{bmatrix} q_1^*(t - T_1) - q_1(t - T_1) \\ q_2^*(t - T_2) - q_2(t - T_2) \\ \vdots \\ q_n^*(t - T_n) - q_n(t - T_n) \end{bmatrix},$$

$T_i > 0$ are the delays. $\mathbf{K_P}$ and $\mathbf{K_R} \in \mathbb{R}^{n\times n}$ are diagonal matrices whose entries are given by $k_{P_i}, k_{R_i} \in \mathbb{R}^+$ for $i = 1, 2, ..., n$ respectively.

Then, the control input torque (11) is now of the form:

$$\tau_{PR} = \mathbf{M}(\mathbf{q})\left[\ddot{\mathbf{q}}^*(t) + \mathbf{K_P}\mathbf{e_q} - \mathbf{K_R}\mathbf{e_q}(t - T_i)\right] + \mathbf{G}(\mathbf{q}), \tag{16}$$

while the closed loop error dynamics looks as:

$$\ddot{\mathbf{e}}_\mathbf{q} + \mathbf{K_P}\mathbf{e_q} - \mathbf{K_R}\mathbf{e_q}(t - T_i) = \mathbf{W_{cd}}, \tag{17}$$

where $\mathbf{W_{cd}}$ was assumed in (14). In the frequency domain, (17) is given by:

$$(s^2\mathbf{I_n} + \mathbf{K_P} - \mathbf{K_R}e^{-s\mathbf{T}})\mathbf{e_q}(s) = \mathbf{W_{cd}}(s). \tag{18}$$

Here, $\mathbf{T}$ is a diagonal matrix with entries $t_{i,i} = T_i \in \mathbb{R}^+$ for $i = 1, 2, ..., n$. For the sake of convenience, the following matrix polynomial is proposed:

$$\mathbf{P_{PR}}(s) = s^2\mathbf{I_n} + 2\Delta s + \mathbf{V} + \tilde{\mathbf{K}} - \mathbf{K_R}e^{-s\mathbf{T}} \tag{19}$$

where the term $2\Delta s$ is associated to the viscous friction and it is considered unknown. The term $\mathbf{V} + \tilde{\mathbf{K}}$ represents the gain matrix $\mathbf{K_P}$ with $\mathbf{V}, \tilde{\mathbf{K}} \in \mathbb{R}^{n\times n}$ diagonal matrices, whose coefficients are of the form $v_{i,i} = v_i^2$, $\tilde{k}_{i,i} = \tilde{\kappa}_i$ and $\Delta_{i,i} = \delta_i v_i$ for $v_i, \tilde{\kappa}_i, \delta_i \in \mathbb{R}^+$ and $i = 1, 2, ..., n$. Where, due to conditions (2)-(6), matrix $\mathbf{W_{cd}}$ is bounded, and according [44], the effects of $\mathbf{W_{cd}}$ can be mitigated by an appropriate selection of the gain matrices $\mathbf{K_P}$ and $\mathbf{K_R}$.

In [29] and [30], tuning rules for the design of proportional-retarded controllers via σ-stabilization are provided. To follow this methodology, let us study the $i-th$ quasi-polynomial of (19):

$$P_{PRi}(s) = s^2 + 2\delta_i v_i s + v_i^2 + \tilde{\kappa}_i - k_{Ri}e^{-sT_i} = 0, \tag{20}$$

and, in order to analyze the σ-stability of the former quasi-polynomial, the change of variable $s \to (s - \sigma_i)$ (for $\sigma_i > 0$) must be applied, then (20) is of the form:

$$\begin{aligned} P_{PR,i}(s - \sigma_i) = {} & s^2 - 2(\sigma_i - \delta_i v_i)s + (\sigma_i - \delta_i v_i)^2 \\ & + v_i^2(1 - \delta_i^2) + \tilde{\kappa}_i - k_{Ri}e^{-(s-\sigma_i)T_i}. \end{aligned} \tag{21}$$

The analysis presented in [30], is intended to obtain the maximal reachable decay rate (denoted by σ_i^*) of the system response, and it is shown that the maximal decay rate is reached when a triple root of the closed loop system is placed at $\sigma_i = \sigma_i^*$. Then, according [29] and [30] this phenomenon occurs when the following conditions holds:

$$\begin{aligned} 0 &= P_{PR,i}(s - \sigma_i)\big|_{s=0} \\ 0 &= \frac{\partial P_{PR,i}(s - \sigma_i)}{\partial s}\bigg|_{s=0} \\ 0 &= \frac{\partial^2 P_{PR,i}(s - \sigma_i)}{\partial s^2}\bigg|_{s=0}. \end{aligned}$$

Then, according [30, Lemma 1], three dominant real roots are placed at $\sigma_i = \sigma_i^*$ and the maximal exponential decay rate σ^* is reached, if the control parameters are selected as follows:

$$\sigma_i^* = \delta_i v_i + \sqrt{v_i^2(1 - \delta_i^2) + \tilde{\kappa}_i}, \tag{22}$$

and, the gain values k_{Pi}, k_{Ri} and delay T_i of the input torque (16) are:

$$k_{Pi} = v_i^2 + \tilde{\kappa}_i, \tag{23}$$

$$T_i = \frac{1}{\sqrt{\nu_i^2(1-\delta_i^2)+\tilde{\kappa}_i}}, \tag{24}$$

$$k_{Ri} = \frac{2(\sigma_i^* - \delta_i \nu_i)}{T_i e^{\sigma_i^* T_i}}. \tag{25}$$

IV. DYNAMIC MODEL AND CONTROLLER DESIGN

This section is devoted to provide the dynamic equations of a 2-DOF planar robot manipulator. Also the proposed design methodology for the PD+G and PR+G control schemes to perform tracking trajectories tasks is presented.

A. DYNAMIC MODEL OF 2-DOF MANIPULATOR ROBOT

In Figure 1 a schematic of the planar robot under study is presented. Here, L_1 and L_2 represent the length of each link, l_1 and l_2 stand for the length of each center of mass, while m_1 and m_2 are the masses of the links, and their inertias are denoted as I_1 and I_2. The gravitational constant is g and finally τ_1 and τ_2 symbolize the control inputs.

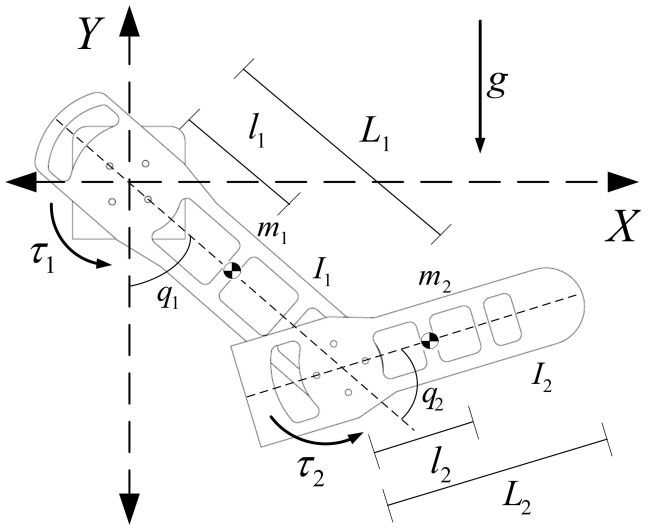

FIGURE 1. 2-DOF robot manipulator scheme.

The generalized coordinates are given by the angular positions $\mathbf{q} = [q_1\ q_2]^T$ and the dynamic model of the robot manipulator is given as follows:

$$\mathbf{M}(\mathbf{q})\ddot{\mathbf{q}} + \mathbf{C}(\mathbf{q},\dot{\mathbf{q}})\dot{\mathbf{q}} + \mathbf{G}(\mathbf{q}) = \tau - \mathbf{D}\dot{\mathbf{q}} \tag{26}$$

where $\tau = [\tau_1\ \tau_2]^T$ represents the generalized input torque vector and:

$$\mathbf{M}(\mathbf{q}) = \begin{bmatrix} m_{11} & m_{12} \\ m_{21} & m_{22} \end{bmatrix},$$

where

$$\begin{aligned} m_{11} &= m_1 l_1^2 + m_2 L_1^2 + m_2 l_2^2 + 2m_2 L_1 l_2 \cos(q_2) + I_1 + I_2 \\ m_{12} &= m_{21} = m_2 l_2^2 + m_2 L_1 l_2 \cos(q_2) + I_2 \\ m_{22} &= m_2 l_2^2 + I_2, \end{aligned}$$

$$\mathbf{C}(\mathbf{q},\dot{\mathbf{q}}) = \begin{bmatrix} -2m_2 L_1 l_2 \dot{q}_2 \sin(q_2) & -m_2 L_1 l_2 \dot{q}_2 \sin(q_2) \\ m_2 L_1 l_2 \dot{q}_1 \sin(q_2) & 0 \end{bmatrix},$$

$$\mathbf{G}(\mathbf{q}) = \begin{bmatrix} (m_1 l_1 + m_2 L_1) g \sin(q_1) + m_2 l_2 g \sin(q_1+q_2) \\ m_2 l_2 g \sin(q_1+q_2) \end{bmatrix},$$

and D is the unknown matrix of the viscous friction and is of the form:

$$\mathbf{D} = \begin{bmatrix} d_1 & 0 \\ 0 & d_2 \end{bmatrix}.$$

B. THE 2-DOF MANIPULATOR ROBOT TRACKING TRAJECTORY PROBLEM

It is desired that the end effector of the planar robot manipulator located at the position:

$$\begin{aligned} x(t) &= L_1 \sin(q_1) + L_2 \sin(q_1+q_2), \\ y(t) &= -L_1 \cos(q_1) - L_2 \cos(q_1+q_2), \end{aligned}$$

follows a predefined trajectory given by the position reference $(x^*(t), y^*(t))$. With the inverse kinematics of the planar robot manipulator, the Cartesian trajectories can be projected as the desired joint trajectories $\left(q_1^*(t), q_2^*(t)\right)$, (see [2]). The set of equations that describes the inverse kinematics is:

$$\begin{aligned} \cos(q_2^*) &= \frac{[x^*(t)]^2 + [y^*(t)]^2 - L_1^2 - L_2^2}{2L_1 L_2}, \\ \sin(q_2^*) &= \sqrt{1-(\cos(q_2^*))^2}, \\ \cos(q_1^*) &= \frac{L_2 \sin(q_2^*)x^*(t) - (L_1 + L_2\cos(q_2^*))y^*(t)}{[x^*(t)]^2 + [y^*(t)]^2}, \\ \sin(q_1^*) &= \frac{(L_1 + L_2\cos(q_2^*))x^*(t) + L_2 \sin(q_2^*)y^*(t)}{[x^*(t)]^2 + [y^*(t)]^2}, \\ q_1^*(t) &= \arctan\left(\frac{\sin(q_1^*)}{\cos(q_1^*)}\right), \\ q_2^*(t) &= \arctan\left(\frac{\sin(q_2^*)}{\cos(q_2^*)}\right). \end{aligned} \tag{27}$$

C. PD+G CONTROL DESIGN

In (11), a Proportional Derivative control scheme [32] is proposed and denoted by:

$$\mathbf{u} = \mathbf{u_{PD}} = -\mathbf{K_P}\mathbf{e_q} - \mathbf{K_D}\dot{\mathbf{e}}_\mathbf{q}, \tag{28}$$

where, $\mathbf{K_P}, \mathbf{K_D} \in \mathbb{R}^{n\times n}$ are diagonal matrices whose entries are given by $k_{Pi}, k_{Di} \in \mathbb{R}^+$ for $i = 1, 2, ..., n$, respectively. In order to reduce the noise amplification problem, which arises by the computation of the joint velocity vector $\dot{\mathbf{q}}$, the error $\dot{\mathbf{e}}_q$ is estimated using a numerical differentiation algorithm plus a low pass filter. Thus, from equation (11), the complete robot arm input torque is now of the form:

$$\tau_{PD} = \mathbf{M}(\mathbf{q})\left[\ddot{\mathbf{q}}^* + \mathbf{K_P}\mathbf{e_q} + \mathbf{K_D}\dot{\mathbf{e}}_\mathbf{q}\right] + \mathbf{G}(\mathbf{q}), \tag{29}$$

while the closed loop error dynamics, looks as:

$$\ddot{\mathbf{e}}_\mathbf{q} + \mathbf{K_D}\dot{\mathbf{e}}_\mathbf{q} + \mathbf{K_P}\mathbf{e_q} = \mathbf{W_{cd}}. \tag{30}$$

The effects of the dynamics of $\mathbf{W_{cd}}$ can be mitigated by an appropriate selection of the gain matrices $\mathbf{K_P}$ and $\mathbf{K_D}$. These gains, are commonly selected using a representation of the tracking error dynamics (30) in the frequency domain, that is:

$$(s^2\mathbf{I} + \mathbf{K_D}s + \mathbf{K_P})\mathbf{e_q}(s) = \mathbf{W_{cd}}(s). \tag{31}$$

Here, one can specify the closed loop characteristic function as a diagonal matrix polynomial of the form:

$$\mathbf{P_{PD}}(s) = s^2\mathbf{I_n} + \mathbf{K_D}s + \mathbf{K_P}. \tag{32}$$

In fact, each of the above polynomials can be proposed in such a way, that its dynamics coincides with that of a stable second order characteristic polynomial. To this aim, the polynomial

$$P_{PDi}(s) = s^2 + 2\zeta_i\omega_{0i}s + \omega_{0i}^2, \tag{33}$$

is proposed, and to match their dynamics, the gains are selected as follows:

$$k_{Pi} = \omega_{0i}^2, \tag{34}$$

$$k_{Di} = 2\zeta_i\omega_{0i}, \quad for\ i = 1, 2, ..., n. \tag{35}$$

where $\zeta_i > 0$ and $\omega_{0i} > 0$.

Now, in order to compute the PD+G control law we use equation (29) with $i = 1, 2$, then input torque is simplified as:

$$\begin{bmatrix} \tau_{1PD} \\ \tau_{2PD} \end{bmatrix} = \mathbf{M}(\mathbf{q}) \times \begin{bmatrix} \ddot{q}_1^* + k_{D1}(\dot{q}_1^* - \dot{q}_1) + k_{P1}(q_1^* - q_1) \\ \ddot{q}_2^* + k_{D2}(\dot{q}_2^* - \dot{q}_2) + k_{P2}(q_2^* - q_2) \end{bmatrix} + \mathbf{G}(\mathbf{q}), \tag{36}$$

where the proportional derivative gains are chosen according (34)-(35) as:

$$k_{P1} = \omega_{01}^2, \quad k_{D1} = 2\zeta_1\omega_{01}, \quad k_{P2} = \omega_{02}^2, \quad k_{D2} = 2\zeta_2\omega_{02}. \tag{37}$$

D. PR+G CONTROL DESIGN

In the same way, in order to compute the PR+G control law, we use equation (16) with $i = 1, 2$ the PR+G input torque is simplified as:

$$\begin{bmatrix} \tau_{1PR} \\ \tau_{2PR} \end{bmatrix} = \mathbf{M}(\mathbf{q}) \begin{bmatrix} \ddot{q}_1^* + k_{R1}(q_1^*(t - T_1) - q_1(t - T_1)) \\ \ddot{q}_2^* + k_{R2}(q_2^*(t - T_2)) - q_2(t - T_2)) \\ +k_{P1}(q_1^* - q_1) \\ +k_{P2}(q_2^* - q_2) \end{bmatrix} + \mathbf{G}(\mathbf{q}), \tag{38}$$

where the gains and the delay of the PR controller are chosen using the set of equations (22)-(25) as:

$$\begin{aligned} \sigma_1^* &= \delta_1\nu_1 + \sqrt{\nu_1^2(1-\delta_1^2) + \tilde{\kappa_1}}, \quad k_{P1} = \nu_1^2 + \tilde{\kappa}_1, \\ T_1 &= \frac{1}{\sqrt{\nu_1^2(1-\delta_1^2) + \tilde{\kappa}_1}}, \quad k_{R1} = \frac{2(\sigma_1^* - \delta_1\nu_1)}{T_1 e^{\sigma_1^* T_1}}, \\ \sigma_2^* &= \delta_2\nu_2 + \sqrt{\nu_2^2(1-\delta_2^2) + \tilde{\kappa_2}}, \quad k_{P2} = \nu_2^2 + \tilde{\kappa}_2, \\ T_2 &= \frac{1}{\sqrt{\nu_2^2(1-\delta_2^2) + \tilde{\kappa}_2}}, \quad k_{R2} = \frac{2(\sigma_2^* - \delta_2\nu_2)}{T_2 e^{\sigma_2^* T_2}}. \end{aligned} \tag{39}$$

The controller gains ν_i and δ_i can be chosen in accordance with a desired closed-loop second order stable polynomial of the form (33). Then, the controller gains can be selected as $\nu_i = \omega_{0i}$ and $0 < \delta_i < 1$. $\tilde{\kappa}_i$ must satisfy $\tilde{\kappa}_i > 0$.

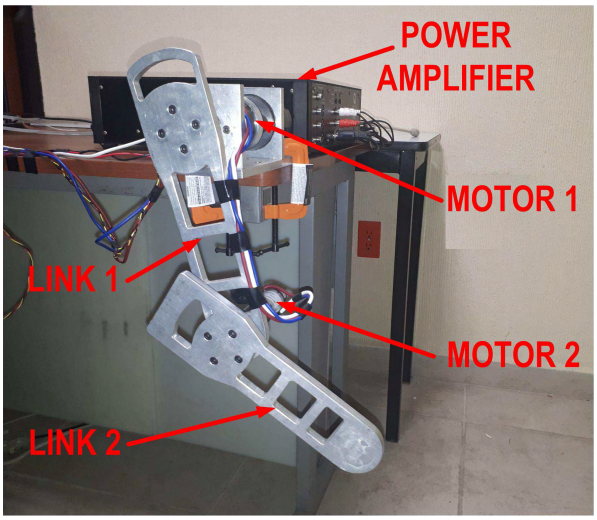

FIGURE 2. Experimental 2-DOF robot manipulator prototype.

V. EXPERIMENTAL RESULTS

Figure 2 shows the robot manipulator experimental platform. The angular position of each link was obtained by means of incremental encoders with resolution of 300 pulses/rotation. While a 24 Volts PHIDGETS motor provides torque to the first link by a gear box with a 1:18 ratio and output maximum torque of 4.412 [N-m] . The second link torque is supplied by a 12 Volts PHIDGETS motor with a gear box with a 1:51 ratio providing a maximum torque of 0.294 [N-m].

A data acquisition board Sensoray Model 626 is responsible of collecting the robot manipulator angular positions and send them to the computer, it also supplies the PWM control signals to a POLOLU H bridge model VNH5019 motor driver. Each of the control schemes was implemented in the Matlab/Simulink platform with a 0.001[s] sample time. The 2-DOF planar robot manipulator parameters are depicted in Table 1.

TABLE 1. Experimental prototype parameters.

Parameter	Value	Parameter	Value
m_1	0.452[Kg]	L_1	0.2 [m]
m_2	0.269[Kg]	L_2	0.18 [m]
l_1	0.122 [m]	I_1	0.0045 [kg m^2]
l_2	0.0447 [m]	I_2	0.00171 [g m^2]

The reference trajectory, in the Cartesian space (X, Y), was proposed as: the initial conditions of the 2-DOF manipulator robot end effector are $t = 0$[s], $x(0) = 0[m]$, $y(0) = -0.38[m]$. Then, when $t = 1.5$[s], the robot follows a smooth trajectory from its initial position to the position, $x^*(3) = 0.34$[m], $y^*(3) = 0$[m], staying in that position for 1[s]. At $t = 4$[s], the reference trajectory is defined by a circumference with center in $(0.21, 0)$[m] and radius equals to 0.13[m] and it is described by $x^*(t) = 0.21 + 0.13\sin(\phi^*(t))$[m] and $y^*(t) = 0.13\cos(\phi^*(t))$[m]. Here $\phi^*(t)$ represents a smooth trajectory from $\phi^*(4) = 0$[rad] to $\phi^*(20) = 2\pi$[rad].

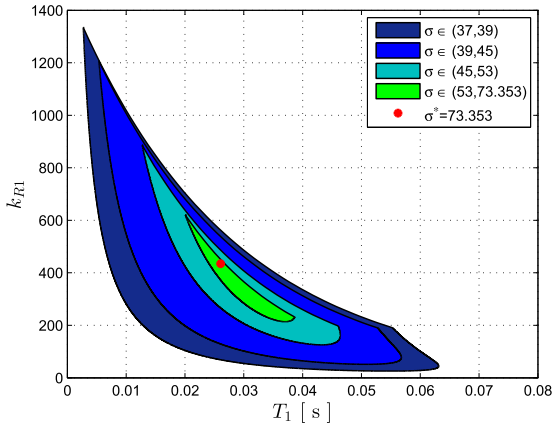

FIGURE 3. σ-stable region for q_1 (simulation).

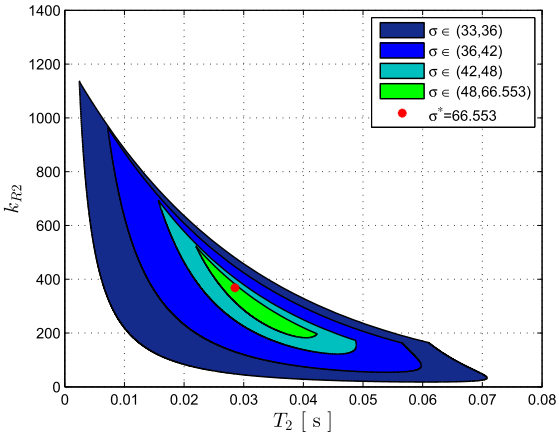

FIGURE 4. σ-stable region for q_2 (simulation).

Finally, the robot returns out to its initial position $x^*(23) = 0[m]$, $y^*(23) = -0.38[m]$. The reference path is shown in Figure 11.

The inverse kinematics presented in (27) is used to compute the desired joint trajectories $\left(q_1^*(t), q_2^*(t)\right)$. The initial conditions for the joint variables are $(0, 0)$. According to (37), the gains of the Proportional Derivative controller were selected as: $\omega_{01} = 50$, $\zeta_1 = 0.7$, $\omega_{02} = 45$, $\zeta_2 = 0.7$. Then, the Proportional Derivative matrices are simplified as:

$$\mathbf{K_P} = \begin{bmatrix} 2500 & 0 \\ 0 & 2025 \end{bmatrix}, \quad \mathbf{K_D} = \begin{bmatrix} 70 & 0 \\ 0 & 63 \end{bmatrix}.$$

Since the velocity vector $\dot{\mathbf{q}}$ is not available, then, a low pass filter with transfer function $G(s) = \frac{300s}{s+300}$, is used to estimate it and to reduce the noise generated by the estimation of the so-called "dirty derivative".

On the other hand, following (39), the gain parameters of the Proportional Retarded controller $\mathbf{u_{PR}}$were chosen as: $\nu_1 = \omega_{01} = 50$, $\delta_1 = 0.7$, $\tilde{\kappa_1} = 196$, $\nu_2 = \omega_{02} = 45$, $\delta_2 = 0.7$, $\tilde{\kappa_2} = 196$, thus, the matrix gains looks as:

$$\mathbf{K_P} = \begin{bmatrix} 2696 & 0 \\ 0 & 2221 \end{bmatrix}, \quad \mathbf{K_R} = \begin{bmatrix} 434.538 & 0 \\ 0 & 368.070 \end{bmatrix}.$$

Figures 3 and 4 show, for q_1 and q_2 respectively, the σ-stability boundaries in the parametric space (k_{Ri}, T_i), where each contour curve corresponds to a value of σ. In each figure, the red mark represents the maximal achievable decay rate σ^* and it represents the place where all the σ-stable boundaries collapse in a single point. For the first joint, the maximum decay rate $\sigma_1^* = 73.353$ is obtained when the controller gains are set as $k_{R1} = 434.538$ and $T_1 = 0.026$[s], while for the second joint, the maximum decay rate is $\sigma_2^* = 66.553$, and is reached with the controller gains established as $k_{R2} = 368.070$ and $T_2 = 0.0285$[s].

Figure 5 depicts the tracking results for the joint q_1, when the planar robot is controlled by the PD+G controller and its behavior, when the PR+G controller is implemented, appears in Figure 6. The tracking errors for both controllers are detailed in the upper subplot of Figure 7. Nevertheless, no

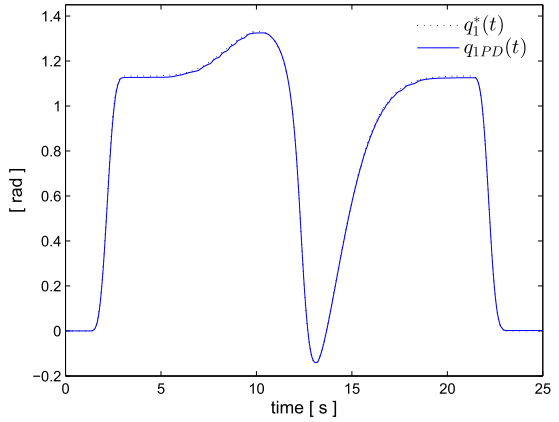

FIGURE 5. PD+G trajectory tracking performance of q_1 (experimental).

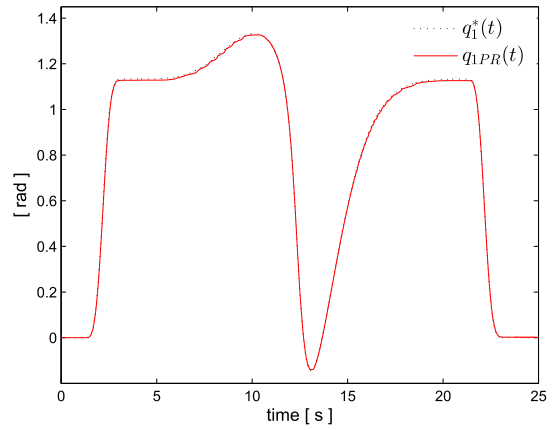

FIGURE 6. PR+G trajectory tracking performance of q_1 (experimental).

conclusion related to the presence of noise can be stated, thus a detailed view of a segment of the error dynamic is presented in the lower subplot of Figure 7. Now, it can be verified that the ripple of the PR controller is lower than the ripple that present the PD controller.

Figures 8 and Figure 9 show the tracking results for the PD+G and PR+G controllers for the second joint q_2. The error tracking performance appears in the upper subplot of

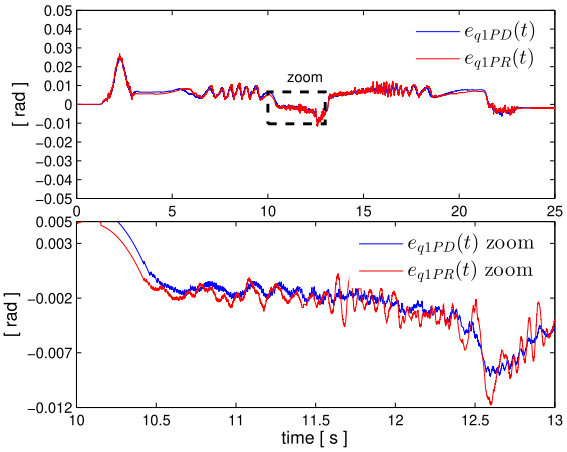

FIGURE 7. q_1 trajectory tracking errors (experimental).

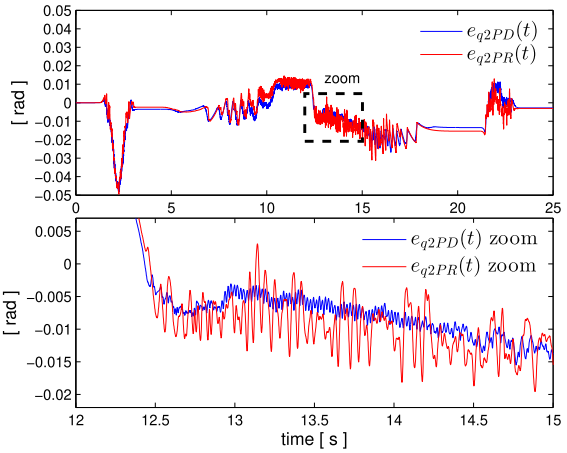

FIGURE 10. q_2 tracking trajectory errors (experimental).

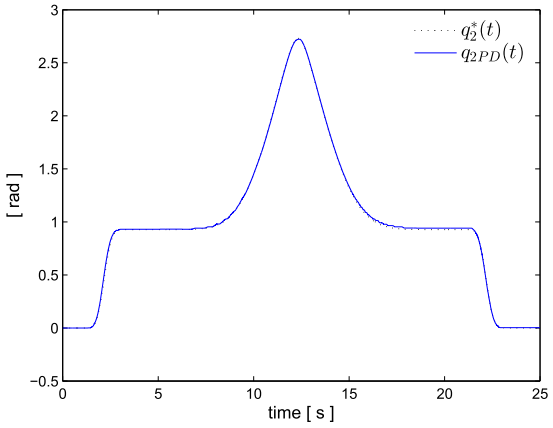

FIGURE 8. PD+G trajectory tracking performance of q_2 (experimental).

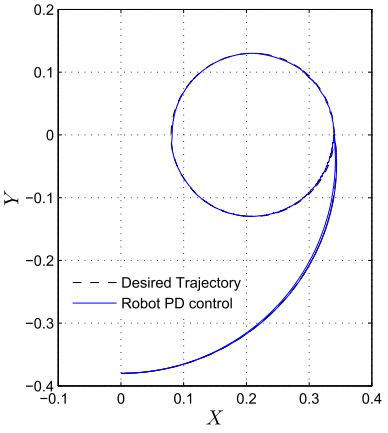

FIGURE 11. PD+G 2-DOF robot trajectory (experimental).

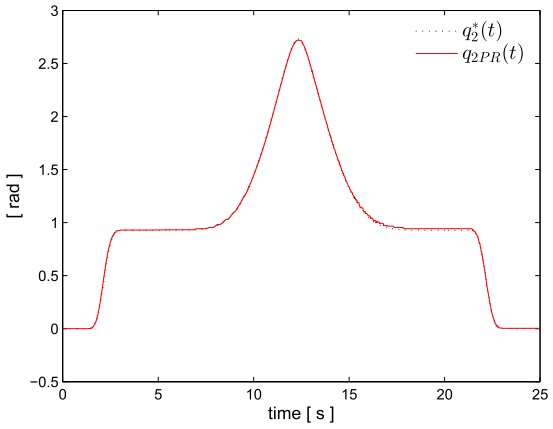

FIGURE 9. PR+G trajectory tracking performance of q_2 (experimental).

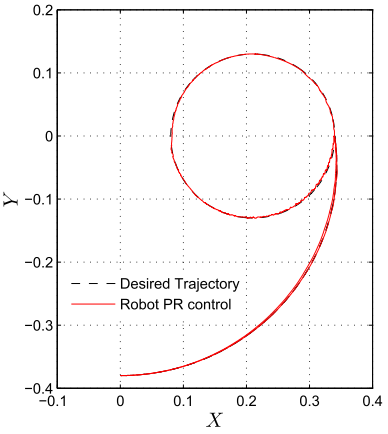

FIGURE 12. PR+G 2-DOF robot trajectory (experimental).

Figure 10, while in the lower subplot a detailed view of a segment of the error dynamics is presented.

The experimental results obtained for PR+G and PD+G in robot joint space task and in the robot Cartesian space for trajectory task (depicted in figures 11 and 12) were satisfactory achieved by both controllers since the tracking errors in both cases are bounded and, from this point of view, the PD+G controller present better results for trajectory tracking tasks. The main difference between PD+G and PR+G experimental results appear in the control effort. Figures 13 and 14, exhibit the applied torque to each joint, where it can be seen that the torque is in the bound of the maximum admissible

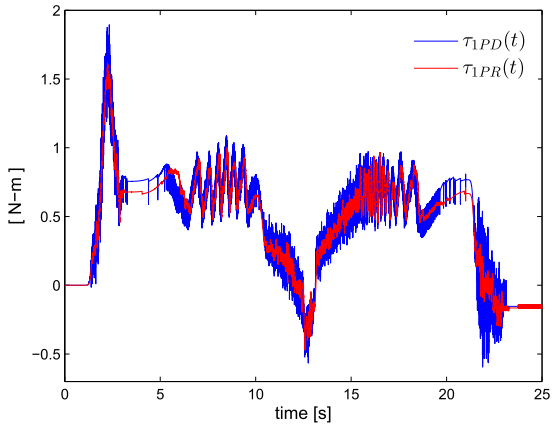

FIGURE 13. q_1 control input (experimental).

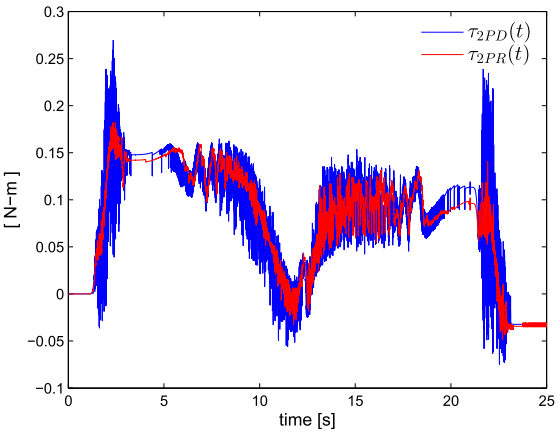

FIGURE 14. q_2 control input (experimental).

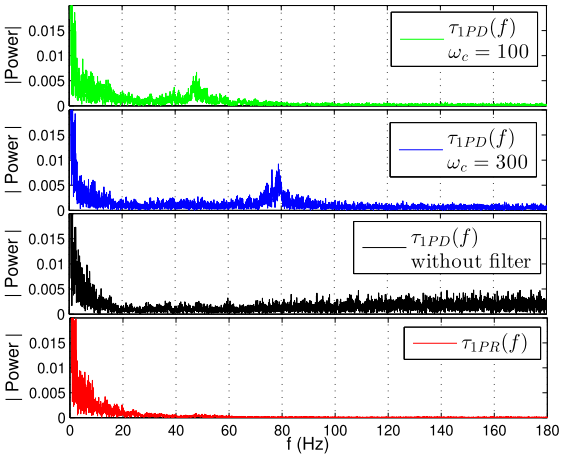

FIGURE 15. τ_1 Frequency spectrum (experimental).

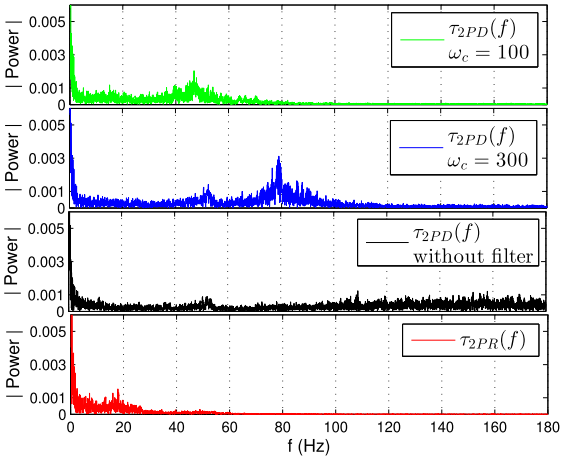

FIGURE 16. τ_2 Frequency spectrum (experimental).

torque provided by actuators, given by $\tau_{1max} = 4.412$ [N-m] and $\tau_{2max} = 0.294$ [N-m]. The PD+G control torque signals are noisier, mainly due to the estimation of the velocity vector $\dot{\mathbf{q}}$ (even with the use of a low pass filter). Then, as a result of this estimation, undesired vibrations appear in the PD+G control law, which can damage the actuators of the robot manipulator or the power electronics stage. In the other hand, the PR+G control torque shows a clear decrease in noise amplitude and frequency, which give us some advantages i.e. easy experimental implementation, less power consumption and vibrations, less wear on the actuators among others.

A frequency spectrum analysis between PR+G and PD+G control is presented in order to explore how the cut-off frequency of the low pass filter $G(s) = \frac{\omega_c s}{s+\omega_c}$ impact on the frequency spectrum of the PD control, three cases are proposed: the nominal case with a cut-off frequency $\omega_c = 300$, the second one considering $\omega_c = 100$, and finally without low pass filter. The first link frequency spectrum results are shown in Figure 15. On the one hand, we can observe that the nominal case $\tau_{1PD}(f)$ $\omega_c = 300$ (blue) exhibits high frequency components with a peak approximately in $f = 80$[Hz], frequencies that commonly are associated with noise, in the same way $\tau_{1PD}(f)$ $\omega_c = 100$ (green) exhibits a high frequency components this case with a peak approximately in $f = 50$[Hz], we can notice if we select the cut-off frequency smaller this peak is moved to the low frequencies, the response of the $\tau_{1PD}(f)$ *withoutfilter* (black) shows that high frequencies are affected the system given as a result undesired oscillations and wear on the actuator. On the other hand, the proposed control $\tau_{1PR}(f)$ shows all its components are concentrated in low frequencies. Similar results can be deduced from Figure 16, where the spectral analysis for the second link is presented. In the nominal case $\tau_{2PD}(f)$ $\omega_c = 300$ presents high frequency components with a peak approximately in $f = 80$[Hz], $\tau_{2PD}(f)$ $\omega_c = 100$ the peak is observed in $f = 50$[Hz], and $\tau_{2PD}(f)$ *withoutfilter* presents high frequencies whereas in the lower figure $\tau_{2PR}(f)$ exhibits low frequency components.

Finally, in order to be able to compare quantitatively the performance of the proposed controllers, a Quadratic Error Index is computed as

$$ISI_{qi}(t) = \int_0^t (q_i - q_i^*)^2 d\tau. \tag{40}$$

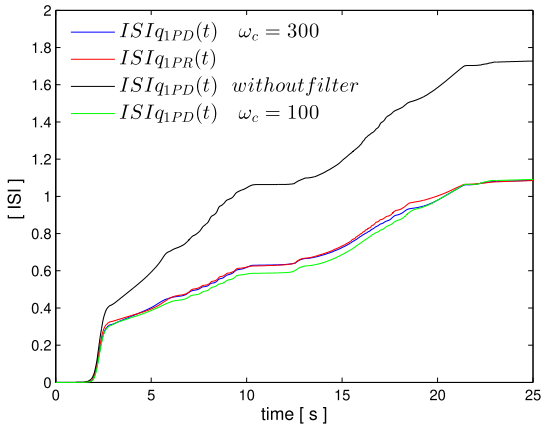

FIGURE 17. q_1 performance index (experimental).

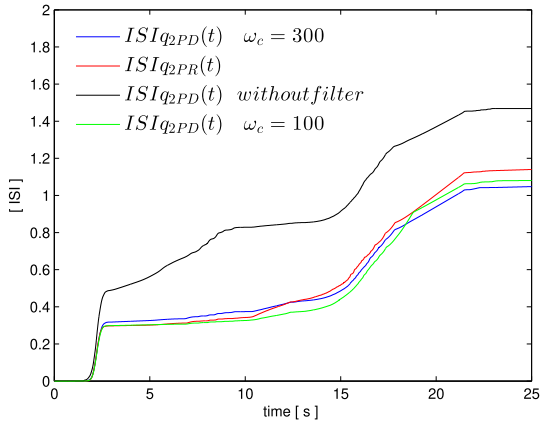

FIGURE 18. q_2 performance index (experimental).

Figure 17 shows the performance index for first link, we can notice that the nominal controller $ISI_{q1PD}(t)$ $\omega_c = 300$ exhibit similar results to $ISI_{q1PD}(t)$ $\omega_c = 100$. where the $ISI_{q1PD}(t)$ $withoutfilter$. shows the worst results and $ISI_{q1PD}(t)$ $\omega_c = 100$ show the best performance, we can notice that the proposed controller $ISI_{q1PR}(t)$ exhibits the performance closer to the nominal case $ISI_{q1PD}(t)$ $\omega_c = 300$. In Figure 18 the second link performance indexes are depicted, both controllers show similar behavior with slightly variations between $ISIq_{2PD}(t)$ and $ISIq_{2PR}(t)$.

VI. CONCLUDING REMARKS

The present manuscript proposes the use of a Proportional Retarded controller plus gravity compensation to overcome the disadvantages that yield the velocity estimation in the Proportional Derivative control in robot manipulators. Indeed, despite of its basic structure, it has been shown (through experimental implementation) that the PR controller is capable of controlling the nonlinear robot dynamics and compensating the possible inherent uncertainties. Although the experimental comparison shows that the PD+G controller shows a better performance in trajectory tasks results (in the sense of the magnitude of the tracking error, and validated by a quadratic error index analysis comparison), the PR+G highlights due it easy implementation, the less noisy torque control signals (validated via an analysis of the frequency spectrum) and its adequate performance in tracking trajectory tasks without the use of signal filtering stages.

REFERENCES

[1] B. Paden and R. Panja, "Globally asymptotically stable 'PD+' controller for robot manipulators," *Int. J. Control*, vol. 47, no. 6, pp. 1697–1712, 1988.
[2] M. W. Spong, S. Hutchinson, and M. Vidyasagar, *Robot Modeling and Control*, vol. 3. New York, NY, USA: Wiley, 2006,
[3] A. Zavala-Río, E. Aguiñaga-Ruiz, and V. Santibáñez, "Global trajectory tracking through output feedback for robot manipulators with bounded inputs," *Asian J. Control*, vol. 13, no. 3, pp. 430–438, 2011.
[4] J. Bowkett and R. Mukherjee, "Comparison of control methods for two-link planar flexible manipulator," in *Proc. Int. Des. Eng. Tech. Conf. Comput. Inf. Eng. Conf.* New York, NY, USA: ASME, 2017, pp. 1–10.
[5] Y. Si, J. Pu, and L. Sun, "A fast terminal sliding mode control of two-link flexible manipulators for trajectory tracking," in *Proc. Chin. Automat. Congr. (CAC)*, 2017, pp. 6387–6391.
[6] J. Z. Sąsiadek, S. Ulrich, and A. Krzyżak, "Trajectory tracking and non-parametric identification of flexible space robot manipulators," in *Proc. 23rd Int. Conf. Methods Models Automat. Robot. (MMAR)*, Aug. 2018, pp. 83–88.
[7] Z.-C. Qiu, C. Li, and X.-M. Zhang, "Experimental study on active vibration control for a kind of two-link flexible manipulator," *Mech. Syst. Signal Process.*, vol. 118, pp. 623–644, Mar. 2019.
[8] K. Lochan, J. P. Singh, B. K. Roy, and B. Subudhi, "Hidden chaotic path planning and control of a two-link flexible robot manipulator," in *Nonlinear Dynamical Systems with Self-Excited and Hidden Attractors*. Cham, Switzerland: Springer, 2018, pp. 433–463.
[9] S.-T. Wu, S.-Q. Tang, and K.-P. Huang, "Vibration attenuation of a two-link flexible arm carried by a translational stage," *J. Vib. Control*, vol. 24, no. 23, pp. 1–15, 2018.
[10] H. Berghuis and H. Nijmeijer, "Robust control of robots using only position measurements," *IFAC Proc. Vol.*, vol. 26, no. 2, pp. 329–334, 1993.
[11] H. Berghuis, H. Nijmeijer, and P. Löhnberg, "Observer design in the tracking control problem of robots," in *Proc. Nonlinear Control Syst. Design*. Amsterdam, The Netherlands: Elsevier, 1992, pp. 197–202.
[12] C. C. De Wit and N. Fixot, "Robot control via robust estimated state feedback," *IEEE Trans. Autom. Control*, vol. 36, no. 12, pp. 1497–1501, Dec. 1991.
[13] C. C. De Wit, N. Fixot, and K. J. Astrom, "Trajectory tracking in robot manipulators via nonlinear estimated state feedback," *IEEE Trans. Robot. Autom.*, vol. 8, no. 1, pp. 138–144, Feb. 1992.
[14] R. Kelly, "A simple set-point robot controller by using only position measurements," *IFAC Proc. Vol.*, vol. 26, no. 2, pp. 527–530, 1993.
[15] S. Nicosia and P. Tomei, "Robot control by using only joint position measurements," *IEEE Trans. Autom. Control*, vol. 35, no. 9, pp. 1058–1061, Sep. 1990.
[16] R. M. May, "Time-delay versus stability in population models with two and three trophic levels," *Ecology*, vol. 54, no. 2, pp. 315–325, 1973.
[17] V. L. Kharitonov and A. P. Zhabko, "Lyapunov–Krasovskii approach to the robust stability analysis of time-delay systems," *Automatica*, vol. 39, no. 1, pp. 15–20, 2003.
[18] K. Gu, K. L. Vladimir, and J. Chen, *Stability of Time-Delay Systems*. Berlin, Germany: Springer, 2003.
[19] W. Michiels and S.-I. Niculescu, *Stability and Stabilization of Time-Delay Systems: An Eigenvalue-Based Approach*. Philadelphia, PA, USA: SIAM, 2007.
[20] E. Fridman, *Introduction to Time-Delay Systems: Analysis and Control*. Basel, Germany: Birkhäuser, 2014.
[21] C. V. Hollot, V. Misra, D. Towsley, and W. Gong, "Analysis and design of controllers for AQM routers supporting TCP flows," *IEEE Trans. Autom. Control*, vol. 47, no. 6, pp. 945–959, Jun. 2002.
[22] C. L. Lai and P. L. Hsu, "Design the remote control system with the time-delay estimator and the adaptive smith predictor," *IEEE Trans. Ind. Informat.*, vol. 6, no. 1, pp. 73–80, Feb. 2010.
[23] T. B. Sheridan, "Space teleoperation through time delay: Review and prognosis," *IEEE Trans. Robot. Autom.*, vol. 9, no. 5, pp. 592–606, Oct. 1993.

[24] S.-I. Niculescu, *Delay Effects on Stability: A Robust Control Approach*, vol. 269. New York, NY, USA: Springer, 2001.
[25] C. Abdallah, P. Dorato, J. Benites-Read, and R. Byrne, "Delayed positive feedback can stabilize oscillatory systems," in *Proc. Amer. Control Conf.*, Jun. 1993, pp. 3106–3107.
[26] S. Han and S. P. Bhattacharyya, "PID controller synthesis using a σ-Hurwitz stability criterion," *IEEE Control Syst. Lett.*, vol. 2, no. 3, pp. 525–530, Jul. 2018.
[27] S.-I. Niculescu, K. Gu, and C. T. Abdallah, "Some remarks on the delay stabilizing effect in siso systems," in *Proc. Amer. Control Conf.*, vol. 3, Jun. 2003, pp. 2670–2675.
[28] R. Villafuerte and S. Mondié, "Tuning the leading roots of a second order DC servomotor with proportional retarded control," *IFAC Proc. Vol.*, vol. 43, no. 2, pp. 337–342, 2010.
[29] S. Mondie, R. Villafuerte, and R. Garrido, "Tuning and noise attenuation of a second order system using proportional retarded control," *IFAC Proc. Vol.*, vol. 44, no. 1, pp. 10337–10342, 2011.
[30] R. Villafuerte, S. Mondié, and R. Garrido, "Tuning of proportional retarded controllers: Theory and experiments," *IEEE Trans. Control Syst. Technol.*, vol. 21, no. 3, pp. 983–990, May 2013.
[31] T. Ortega-Montiel, R. Villafuerte-Segura, C. Vázquez-Aguilera, and L. Freidovich, "Proportional retarded controller to stabilize underactuated systems with measurement delays: Furuta pendulum case study," *Math. Problems Eng.*, vol. 2017, Dec. 2017, Art. no. 2505086.
[32] F. L. Lewis, D. M. Dawson, and C. T. Abdallah, *Robot Manipulator Control: Theory and Practice*. Boca Raton, FL, USA: CRC Press, 2003.
[33] L. Sciavicco and B. Siciliano, *Modelling and Control of Robot Manipulators*. Berlin, Germany: Springer, 2012.
[34] R. Ortega, J. A. L. Perez, P. J. Nicklasson, and H. J. Sira-Ramirez, *Passivity-Based Control of Euler-Lagrange Systems: Mechanical, Electrical and Electromechanical Applications*. Berlin, Germany: Springer, 2013.
[35] M. A. Arteaga and R. Kelly, "Robot control without velocity measurements: New theory and experimental results," *IEEE Trans. Robot. Autom.*, vol. 20, no. 2, pp. 297–308, Apr. 2004.
[36] P. R. Belanger, "Estimation of angular velocity and acceleration from shaft encoder measurements," in *Proc. IEEE Int. Conf. Robot. Automat.*, May 1992, pp. 585–592.
[37] F. Janabi-Sharifi, V. Hayward, and C.-S. J. Chen, "Discrete-time adaptive windowing for velocity estimation," *IEEE Trans. Control Syst. Technol.*, vol. 8, no. 6, pp. 1003–1009, Nov. 2000.
[38] P. R. Belanger, P. Dobrovolny, A. Helmy, and X. Zhang, "Estimation of angular velocity and acceleration from shaft-encoder measurements," *Int. J. Robot. Res.*, vol. 17, no. 11, pp. 1225–1233, 1998.
[39] G. Liu, "On velocity estimation using position measurements," in *Proc. Amer. Control Conf.*, vol. 2, May 2002, pp. 1115–1120.
[40] Y. X. Su, C. H. Zheng, P. C. Müller, and B. Y. Duan, "A simple improved velocity estimation for low-speed regions based on position measurements only," *IEEE Trans. Control Syst. Technol.*, vol. 14, no. 5, pp. 937–942, Sep. 2006.
[41] W. Yu and X. Li, "PD control of robot with velocity estimation and uncertainties compensation," in *Proc. IEEE 40th Conf. Decis. Control*, vol. 2, Dec. 2001, pp. 1162–1167.
[42] H. Sira-Ramírez, C. López-Uribe, and M. Velasco-Villa, "Linear observer-based active disturbance rejection control of the omnidirectional mobile robot," *Asian J. Control*, vol. 15, no. 1, pp. 51–63, 2013.
[43] R. Madoński and P. Herman, "Survey on methods of increasing the efficiency of extended state disturbance observers," *ISA Trans.*, vol. 56, pp. 18–27, May 2015.
[44] T. Kailath, *Linear Systems*, vol. 156. Upper Saddle River, NJ, USA: Prentice-Hall, 1980.

MARIO RAMÍREZ-NERIA received the B.S. degree in mechatronics engineering from UPIITA-IPN, National Polytechnic Institute, Mexico City, Mexico, the M.S. degree in electrical engineering from the Mechatronics Section, Electrical Engineering Department, CINVESTAV-IPN, Mexico City, and the Ph.D. degree from the Automatic Control Department, CINVESTAV-IPN. His current research interests include the applications of control theory, active disturbance rejection control, mechanical underactuated systems, and robotics.

GILBERTO OCHOA-ORTEGA was born in Mexico City, Mexico, in 1979. He was graduated from the National Polytechnic Institute, Mexico, in 2003. He received the master's and Ph.D. degrees from the Automatic Control Department, CINVESTAV, in 2006 and 2010, respectively. Since 2009, he has been with the Division of Mechatronics, Polytechnic University of the Valley of Mexico. His research interests include time-delay systems, linear systems, and control of mechatronics systems.

ALBERTO LUVIANO-JUÁREZ was born in Mexico City, Mexico, in 1981. He received the B.S. degree in mechatronics engineering from the National Polytechnic Institute (IPN), Mexico, in 2003, the M.Sc. degree in automatic control from the Automatic Control Department, CINVESTAV, IPN, in 2006, and the Ph.D. degree in electrical engineering from the Mechatronics Section, Department of Electrical Engineering, CINVESTAV, in 2011. Since 2011, he has been with the Postgraduate and Research Section, UPIITA-IPN. His research interests include robust estimation and control in mechatronic systems, robotics, and algebraic methods in the estimation and control of mechatronic systems.

NORMA LOZADA-CASTILLO was graduated from the Superior School of Physics and Mathematics (ESFM), National Polytechnic Institute (IPN). She received the master's and Ph.D. degrees from the Automatic Control Department, CINVESTAV, IPN. Her research interests include stochastic control, non-linear control, and estimation in stochastic systems.

MIGUEL ANGEL TRUJANO-CABRERA was born in Mexico City, Mexico, in 1982. He received the B.S. degree in mechatronics engineering from the National Polytechnic Institute, in 2005, and the M.Sc. and Ph.D. degrees in automatic control from the Department of Automatic Control, CINVESTAV, in 2008 and 2012, respectively. Since 2013, he has with the Division of Mechatronics, Polytechnic University of the Valley of Mexico. His research interests include robotics, artificial vision, and mechatronic systems.

JUAN PABLO CAMPOS-LÓPEZ was born in Mexico City, Mexico, in 1982. He received the B.S. degree in mechanic engineering from UNAM, in 2005, and the M.Sc. and Ph.D. degrees in mechanical engineering from the National Polytechnic Institute, in 2008 and 2012, respectively. Since 2012, he has been with the Division of Mechatronics, Polytechnic University of the Valley of Mexico. His research interests include mechatronics systems, and strain measurements with noninvasive techniques.